

Diffusion of liquid domains in lipid bilayer membranes

Pietro Cicuta,¹ Sarah L. Keller,² and Sarah L. Veatch³,

¹Cavendish Laboratory and Nanoscience Center, University of Cambridge, Cambridge CB3 0HE, U.K.

²Departments of Chemistry and Physics, University of Washington, Seattle, WA 98195-1700, USA

³Department of Microbiology and Immunology, University of British Columbia, Vancouver, BC, V6T 1Z4, Canada

We report diffusion coefficients of micron-scale liquid domains in giant unilamellar vesicles of phospholipids and cholesterol. The trajectory of each domain is tracked, and the mean square displacement grows linearly in time as expected for Brownian motion. We study domain diffusion as a function of composition and temperature, and measure how diffusion depends on domain size. We find mechanisms of domain diffusion which are consistent with membrane-dominated drag in viscous L_o phases [P.G. Saman and M. Delbruck, PNAS 72, 3111 (1975)], and bulk-dominated drag for less viscous L_u phases [B.D. Hughes et al., J. Fluid Mech. 110, 349 (1981)]. Where applicable, we obtain the membrane viscosity and report activation energies of diffusion.

PACS numbers: 68.35.Fx, 68.55.Ac, 87.16.Dg

Diffusion of domains within cell membranes is a highly relevant biophysical problem. The presence of lipid domains, including rafts, can affect both short-range (intra-domain) and long-range (inter-domain) diffusion of membrane components [1, 2]. Diffusion has been observed in live cell membranes [3, 4], although interpreting results from these complex systems can be challenging.

Even in simple model systems, deciphering the diffusion of membrane inclusions is a long-standing and difficult hydrodynamic problem [5, 6, 7]. Objects that diffuse in the membrane plane range from small peptides and individual lipids to large inclusions like protein aggregates and lipid domains. The first challenge is that, unlike in three dimensional (3D) diffusion, the size of the diffusing object is not the only length-scale that enters into the problem. For example, the membrane has finite thickness, a finite surface area, and often a nonzero curvature. Secondly, the membrane is composed of macromolecules, which limits continuum approaches to large objects. Lastly, the membrane and its surroundings have different viscosities. In complex biological membranes, additional length-scales may be important, such as the distance between membrane proteins [8] or the size of corrals created by the actin cytoskeleton [3].

In this Letter, we directly measure diffusion of liquid domains in giant unilamellar vesicles (GUVs) of radius $\sim 20 \mu\text{m}$ as in Figure 1. These domains are micron-scale, circular, span the lipid bilayer, and undergo Brownian motion. By measuring diffusion of bilayer domains over a wide parameter range of more than one decade in domain radii and three decades in 2D membrane viscosities, we probe the two limiting models of Saman-Delbruck [5] and Hughes et al. [6]. We find a cross-over between the two models which would not have been predicted from previous monolayer results [11]. In the cases where our data are well fit by the Saman-Delbruck equation, we are able to extract viscosities of lipid phases and diffusion activation energies.

Domains move in a background phase with two dimen-

sional (2D) membrane viscosity (η). The diffusion coefficient of a membrane inclusion was originally described by Saman and Delbruck [5]:

$$D(r) = \frac{k_B T}{4 \eta} \log \frac{\eta}{\eta_0} \frac{1}{r} + \frac{1}{2} ; \quad (1)$$

where r is the radius of the inclusion, $\eta_0 = 0.5772$ and we have chosen boundary conditions appropriate for liquid domains in a liquid membrane to yield the factor of $1/2$. A key parameter in the hydrodynamics of this system is the lengthscale ℓ_0 defined by the ratio of the membrane η to the 3D bulk viscosity of water (η_w) such that $\ell_0 = \eta/\eta_w$. Eq. 1 is expected to hold for $r < \ell_0$, i.e. small domains and/or large membrane viscosity. Later work confirmed this calculation and derived a result for the

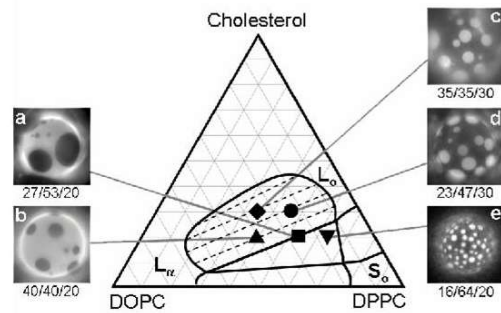


FIG. 1: Fluorescence microscopy phase diagram of DOPC/DPPC/cholesterol and vesicle images at 20°C. Semi-quantitative dashed tie-lines cross the L_u - L_o coexistence region [9]. Some vesicles studied have a continuous L_u (bright) phase (a-b) whereas others have a continuous L_o (dark) phase (c-d). One composition (e) has a continuous dark L_o phase which may contain both L_o and gel (S_o) phase lipids [10]. Vesicle compositions are shown as mol% DOPC/DPPC/Chol.

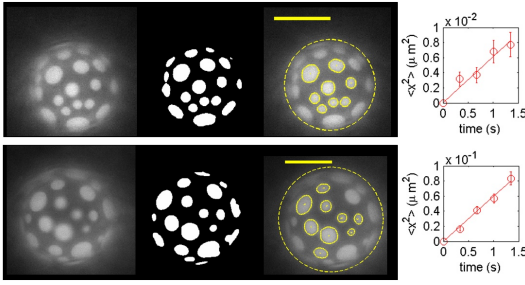


FIG. 2: Greyscale fluorescence images (left) are filtered and thresholded (middle). White regions are identified as domains. Those within a specified size range, ellipticity and distance from the edge are retained. Circles (right image) identify those domains successfully identified through 5 successive frames. Mean square displacement data for domains with radii of 1-1.5 μm are shown at right. Both vesicles have composition 1:2 DOPC:DPPC + 30% Chol, $T = 10$ °C (top) and 20 °C (bottom). Note the factor of ten difference in diffusion coefficients. The scale bar is 40 μm .

opposite limit of $r_0 < r$ [6]:

$$D(r) = \frac{k_B T}{16 \pi \eta r} \quad (2)$$

It is important to notice that for $r_0 < r$ the diffusion coefficient is more strongly dependent on the inclusion's radius, but is independent of the membrane viscosity. This case was verified experimentally through observations of micron-scale domains in monolayers [11]. Other theoretical work has addressed different inclusion shapes as well as large domains [12].

Spherical giant unilamellar vesicles (GUVs; 30-100 μm diameter) are made by electroformation [13] of a ternary mixture of cholesterol with phospholipids of both high (DPPC; di(16:0)PC) and low (DOPC; di(18:1)PC) melting temperatures. Materials and methods have been described previously [10]. The vesicle membranes are initially uniform at high temperature, and phase separate into two liquid phases when vesicle suspensions are placed on a pre-cooled microscope stage. The less viscous L phase is labeled by fluorescent dye (Texas Red-DPPE). The composition and viscosity of the two phases depend on the composition and temperature of the entire vesicle. With time, domains coalesce, allowing us to probe a range of domain sizes at constant temperature.

We probe vesicle lipid compositions in the ternary system of DOPC/DPPC/Chol, as in Figure 1. In previous microscopy and 2H NMR measurements, we established that vesicles with these vesicle compositions separate into a liquid-ordered (L_o) phase rich in the saturated lipid DPPC and a liquid crystalline (L_d) phase rich in the unsaturated lipid DOPC [10, 14]. Two of the vesicle compositions contain a continuous bright L_d phase (Figure 1a-b), and two contain a continuous dark L_o phase (Figure 1c-d). One composition falls within a three phase region (Figure 1e.) The presence of three phases is clear in

2H NMR experiments (manuscript in preparation), but is difficult to detect by microscopy. We probe the viscosity of the continuous phase by tracking domains of the minority phase.

Membrane domains are identified by an image processing program written in Matlab (Figure 2). A Gaussian filter is applied to images before thresholding, to identify features in the size range of domains. Almost no domains are lost by this algorithm. Domains are accepted if: a) the diameter falls between a minimum (2 pixel) and maximum value; b) the shape is circular, such that all points in the domain perimeter lie within 20% of the mean domain radius; and c) the center of mass lies within a circle defined by 0.8 of the vesicle radius. Since all domains are round (shape fluctuations are minimal), these criteria discriminate against occasional problems arising from image analysis filtering (for example, two domains very close to each other will not be accepted).

A separate program tracks domain trajectories with logic similar to existing codes, i.e. by matching a domain with the nearest feature in the next image [15]. Average diffusion is subtracted to yield unbiased domain motion. Matching generates no false positives but does not have a perfect success rate. We therefore divide each movie (typically 100 frames at 0.34 s/frame) into 20 sets of 5 frames over which most domains are tracked successfully. Domain size does not change over this period. The average of vertical and horizontal mean square displacements ($\langle \Delta x^2 \rangle$) is linear with time and $\langle \Delta x^2 \rangle = 2D(r)t$ as expected for diffusion. Over five frames, the MSD is $0.03 \mu m^2$ which is much smaller than the particle separation, and we see no effect of domain packing.

Figure 3 shows diffusion coefficients as a function of domain size. The data has been culled to report only sets in which wide ranges of domain sizes are observed for any fixed temperature and composition. The dashed lines in Figure 3 show the asymptotic $1/r$ behavior given in Eq. 2. Within error, all data fall on or below this theoretical upper bound in diffusion coefficient. Eq. 2 is independent of membrane viscosity and holds when membrane viscosity is low, or domain radius is large i.e. when $r_0 < r$ [6]. For the low viscosity L_d phase (e.g. Figure 3d), it can be seen that the conditions of low membrane viscosity and large domain radius are met through most of the temperature range, because most data fall along the dashed line.

All data below the dashed line in Figure 3 correspond to membranes with high viscosity, notably L_o phases at low temperatures. We have chosen to plot our data to the Saman-Debruck equation, which should hold when membrane viscosity is high. It is clear that this set of data does not have a $D(r) \propto r^{-1}$ dependence, and we find instead reasonable fits to Eq. 1 with a single fitting parameter (η^0). Since our domain radii are limited to 0.5 μm by our optical resolution and 10 μm by our vesicle diameters, we cannot prove that Eq. 1 is the only

Figure 4 demonstrates that domains diffuse in membranes of high viscosity via an activated process. If the 2D membrane viscosity (η) were independent of T , we would expect $D_0(T) \propto T^{-1}$. Instead, we find a better fit for $\log(D_0(T)) \propto T^{-1}$, consistent with an activation energy E_a for diffusion such that $D_0 \propto \exp(-E_a/k_B T)$. The data in Figure 4 follow Arrhenius behavior even though a gel phase emerges at low temperature for some mixtures. Composition of the L_o phase varies only slightly with temperature [10]. Activation energies for individual lipids [22, 23, 24] have been attributed to the energy required to hop into an available free volume [7, 24]. Larger particles such as protein aggregates yield lower apparent activation energies [17]. Fig. 4 lists activation energies for domains diffusing in L_o phases. We find activation energies greater than those reported for single molecules in similar membranes, including DPPC/Chol membranes at high temperature (30–80 kJ/mol) [22], as well as L_o lipids in phase separated DOPC/DPPC/Chol membranes at low temperature (~ 80 kJ/mol) [25].

In summary, we present a simple method for quantifying the movement of domains in membranes with co-existing liquid phases. We find that domains diffuse via Brownian motion, and that diffusion rates are described by different models under different experimental conditions. At high temperatures and in membranes with a continuous L phase, membrane viscosity is low, diffusion constants are independent of membrane properties, and domains diffuse with a radial dependence of $D \propto 1/r$. In membranes with a higher viscosity continuous phase, domain movement does depend on membrane physical properties and the radial dependence can be fitted by a Saman-Debruck model with $D \propto \log(1/r)$. For these membranes, we determine 2D viscosities and report activation energies for domain diffusion.

PC was funded by the Oppenheimer Fund, EPSRC, and the Cavendish-KAIST Cooperative Research Program of MOST Korea. SLK acknowledges an NSF CAREER award and a Cottrell Scholar award. SLV acknowledges a grant from the Cancer Research Institute. We thank Imran Hasnain for help with image analysis, and Klaus Gawrisch for helpful conversations.

veatch@cm.druhc.ca

- [1] D. V. J. Nicolau, K. Burrage, R. G. Parton, and J. F. Hancock, *Mol. Cell Biol.* 26, 313 (2006).
- [2] D. Mader, M. J. Moreno, P. Verkade, W. L. Vaz, and K. Simons, *Proc. Natl. Acad. Sci. USA* 103, 329 (2006).
- [3] A. Kusumi and K. Suzuki, *Biochim. Biophys. Acta* 1746, 234 (2005).
- [4] A. K. Kenworthy, B. J. Nichols, C. L. Remmert, G. M. Hendrix, M. Kumar, J. Zimmerberg, and J. Lippincott-Schwartz, *J. Cell Biol.* 165, 735 (2004); Y. Chen, B. Yang, and K. Jacobson, *Lipids* 39, 1115 (2004); K. Bacia, D. Scherfeld, N. K. Ahya, and P. Schwille, *Biophys. J.* 87, 1034 (2004).
- [5] P. Saman and M. Debruck, *Proc. Natl. Acad. Sci.* 72, 3111 (1975).
- [6] B. D. Hughes, B. A. Pailthorpe, and L. R. White, *J. Fluid Mech.* 110, 349 (1981).
- [7] R. M. Clegg and W. L. C. Vaz, in *Progress in Protein-Lipid Interactions*, edited by Watts and De Pont (Elsevier, 1982).
- [8] M. J. Saxton, *Biophys. J.* 66, 394 (1994).
- [9] Quantitative tie-lines are determined by ^2H NMR (manuscript in preparation). Fluorescence microscopy phase boundaries differ from those determined by ^2H NMR due to the presence of probe lipid.
- [10] S. L. Veatch and S. L. Keller, *Phys. Rev. Lett.* 89, 268101 (2002); S. L. Veatch and S. L. Keller, *Biophys. J.* 85, 3074 (2003); S. L. Veatch and S. L. Keller, *Biochim. Biophys. Acta* 1746, 172 (2005).
- [11] J. F. Klingler and H. M. McConnell, *J. Phys. Chem.* 97, 6096 (1993).
- [12] H. A. Stone and A. Ajdari, *J. Fluid Mech.* 369, 151 (1998); A. J. Levine, T. B. Liverpool, and F. C. MacKintosh, *Phys. Rev. Lett.* 93, 038102 (2004); *ibid*, *Phys. Rev. E* 69, 021503 (2004).
- [13] M. I. Angelova, S. Soleau, P. Meleard, J. F. Faucon, and P. Bothorel, *Progr. Colloid Polym. Sci.* 89, 127 (1992).
- [14] S. L. Veatch, I. V. Polozov, K. Gawrisch, and S. L. Keller, *Biophys. J.* 86, 2910 (2004).
- [15] J. C. Crocker and D. G. Grier, *J. Coll. Int. Sci.* 179, 298 (1996); We track only features identified on the first frame of a set of images. We do not need to track "new" features because movie segments are short and features in 2D remain in the field of view. In contrast, colloidal particles in 3D can leave the field of focus.
- [16] Y. Gambin, R. Lopez-Esparza, M. Reay, E. Sierecki, N. S. Gov, M. Genest, R. S. Hodges, and W. Urbach, *Proc. Natl. Acad. Sci.* 103, 2098 (2006).
- [17] C. Lee, M. Revington, S. Dunn, and N. Petersen, *Biophys. J.* 84, 1756 (2003).
- [18] S. J. Plowman, C. Muncke, R. G. Parton, and J. F. Hancock, *Proc. Natl. Acad. Sci.* 102, 15500 (2005). A. Pralle, P. Keller, E. L. Florin, K. Simons, and J. K. Horber, *J. Cell Biol.* 148, 997 (2000). P. Sharma, R. Varm, R. C. Sarasij, Ira, K. Gousset, G. Krishnamoorthy, M. Rao, and S. May, *Cell* 116, 577 (2004).
- [19] C. F. Brooks, G. G. Fuller, C. W. Curtis, and C. R. Robertson, *Langmuir* 15, 2450 (1999).
- [20] W. Vaz, J. Stempel, D. Hallman, A. Gamboa, and M. D. Rosa, *Eur. Biophys. J.* 15, 111 (1987).
- [21] R. Peters and R. Cherry, *Proc. Natl. Acad. Sci. USA* 14, 4317 (1982); C. Chang, H. Takeuchi, T. Ito, K. Machida, and S. Ohnishi, *J. Biochem.* 90, 997 (1981).
- [22] H. A. Scheidt, D. Huster, and K. Gawrisch, *Biophys. J.* 89, 2504 (2005).
- [23] A. Filippov, G. Ordd, and G. Lindblom, *Biophys. J.* 84, 3079 (2003).
- [24] P. F. Almeida, W. L. C. Vaz, and T. E. Thompson, *Biochemistry* 31, 6739 (1992).
- [25] G. Ordd, P. W. Westerman, and L. G., *Biophys. J.* 89, 315 (2005).